

# Use of point source models for the dispersion of releases of finite size

P.L. Thibaut Brian, Gene K. Lee \*

*Air Products and Chemicals, 7201 Hamilton Blvd., Allentown, PA 18195, USA*

Received 28 February 1997; received in revised form 31 October 1997; accepted 1 November 1997

---

## Abstract

If the releases are of finite size, the point source model is widely accepted as an approximation to the concentration in the far field. However, substantial improvement upon the point source model can be achieved by shifting the origin of the point source release to a virtual origin, a point upwind of the origin of the finite size release. In this paper, rigorous solutions for the finite size release models are compared against the point source model to determine the optimum virtual origin shift so as to produce the most accurate approximation in the intermediate and far fields. Also, the effects of anisotropic diffusion are considered in order to model atmospheric diffusion more closely. © 1998 Elsevier Science B.V.

*Keywords:* Point source model; Virtual origin; Virtual source; Anisotropic diffusion; Atmospheric dispersion; Finite size release

---

## 1. Introduction

Point source models are widely used to assess the consequences of releases of toxic and flammable materials to the atmosphere. If the releases are of finite size, it is understood that the point source model is not a good approximation to the concentration in the near field, but it is widely accepted as an approximation to the concentration in the far field. In many situations there is interest in accurately modeling the concentration in the intermediate field. These include situations in which a ‘top hat’ model, including initial momentum or buoyancy, is to be blended into an atmospheric dispersion model after these effects have subsided. In such cases, substantial improvement can be

---

\* Corresponding author. Tel.: +1 610 481 6424; fax.: +1 610 481 5224; e-mail: leegk@apci.com

achieved by shifting the origin of the point source release to a virtual origin, a point upwind of the origin of the finite size release. This allows for some dispersion of the point source release so that it may grow to the ‘same size’ as the finite size release at the point of origin of the latter.

The use of a virtual origin has been discussed by a number of previous authors [1–4]. Holland [1] appears to have been the first. He suggested shifting the virtual origin so that the center point concentration of the shifted point source solution would be equal to the uniform concentration in the release of finite size. Gifford [2] suggested that a more useful approach would be to shift the virtual origin such that a given percentage of the moles of pollutant in the shifted point source release would be contained within a radius equal to the radius of the finite size release. Gifford does not, however, present a rational approach to selecting this percentage; he mentions 50% and 99%, but he does not recommend any value. Turner [3] and Bowers et al. [4] considered releases of rectangular shape and approximated the shape with a Gaussian profile having an initial standard deviation such that the concentration at the edge of the rectangle becomes arbitrarily one-tenth the centerline concentration. The virtual origin shift is then found that allows the standard deviation for the point source to grow to this value at the true origin of release. The focus of this paper is upon puff releases of spherical shape and continuous release of circular cross section with a uniform concentration over a finite radius. The objective is to determine the optimum virtual origin shift so as to produce the most accurate approximation in the intermediate and far fields. A further objective is to consider the effects of anisotropic diffusion in order to model atmospheric diffusion more closely.

## 2. Theory

### 2.1. Spherical puff release

Consider the release of a spherical puff of radius  $a$  of uniform concentration  $c_0$ . Assuming that the buoyancy and the initial momentum of the release are negligible, the dispersion process can be modeled by the diffusion equation:

$$\frac{\partial}{\partial x} \left( D_x \left( \frac{\partial c}{\partial x} \right) \right) + \frac{\partial}{\partial y} \left( D_y \left( \frac{\partial c}{\partial y} \right) \right) + \frac{\partial}{\partial z} \left( D_z \left( \frac{\partial c}{\partial z} \right) \right) = \frac{\partial c}{\partial t}. \quad (1)$$

At first the diffusivity will be assumed to be isotropic and constant. Atmospheric dispersion shows several significant deviations from this model, and these will be discussed later. The solution is given by Carslaw and Jaeger [5]:

$$c = \frac{1}{2} \left[ \operatorname{erf} \frac{R+1}{2\sqrt{\theta}} - \operatorname{erf} \frac{R-1}{2\sqrt{\theta}} \right] + \frac{1}{R} \sqrt{\frac{\theta}{\pi}} \left[ \exp \frac{-(R+1)^2}{4\theta} - \exp \frac{-(R-1)^2}{4\theta} \right]. \quad (2)$$

At  $R = 0$ ,

$$C^* = \operatorname{erf}\left(\frac{1}{2\sqrt{\theta}}\right) - \frac{1}{\sqrt{\pi\theta}} \exp\left(-\frac{1}{4\theta}\right). \quad (3)$$

For the release of  $Q$  moles in a point source of infinite concentration, the solution is

$$c = \frac{Q}{(2\pi)^{3/2} \sigma^3} \exp\left(-\frac{r^2}{2\sigma^2}\right), \quad (4)$$

where

$$\sigma = \sqrt{2Dt}. \quad (5)$$

Taking the moles released to be the same as in the finite size release,

$$Q = \frac{4}{3} \pi a^3 c_o. \quad (6)$$

The point source solution, in dimensionless form, becomes

$$C = \frac{1}{6\sqrt{\pi} \theta^{3/2}} \exp\left(-\frac{R^2}{4\theta}\right). \quad (7)$$

At  $R = 0$ ,

$$C^* = \frac{1}{6\sqrt{\pi}} \frac{1}{\theta^{3/2}}. \quad (8)$$

The shifted point source solution is obtained by replacing, in Eqs. (7) and (8),  $\theta$  by  $\theta + \theta_s$ . Thus the origin of the point source release is taken to be earlier in time (i.e. upwind), by the amount  $\theta_s$ , than the origin of the finite size release under consideration. The center point concentration then becomes

$$C^* = \frac{1}{6\sqrt{\pi}} \frac{1}{(\theta + \theta_s)^{3/2}}. \quad (9)$$

Similarly, Eq. (5) becomes:

$$\frac{\sigma}{a} = \sqrt{2(\theta + \theta_s)}. \quad (10)$$

Series expansions of the finite size and point source results, given by Eqs. (3) and (9), indicate that asymptotic agreement is obtained by choosing  $\theta_s$  equal to 0.1. For a number of different values of  $\theta$ ,  $C^*$  was calculated using Eq. (3), and the calculated value of  $C^*$  was substituted into Eq. (9), which was then solved for  $\theta_s$ . The results obtained are shown in Table 1. It can be seen that the calculated value of  $\theta_s$  declines and asymptotically approaches 0.1.

Fig. 1 displays the center point concentration,  $C^*$ , vs. dimensionless time,  $\theta$ , for the finite size solution, the point source solution, and the shifted point source solution. The time shift,  $\theta_s = 0.1$ , can be seen to result in a substantial improvement in the accuracy of the point source solution. From a practical point of view, some may prefer an even

Table 1  
Time shift for spherical diffusion

$\theta$	$C^*$ from Eq. (3)	$\theta_s$ from Eq. (9)
0.01	1.000000	0.19678
0.1	0.8282029	0.13447
1	0.08110856	0.10358
2	0.03085964	0.10179
4	0.01132287	0.10089
10	0.00292934	0.10034
20	0.00104346	0.10012
40	0.000370302	0.10006

greater shift. If  $\theta_s$  is chosen to be 0.11, the shifted point source solution declines more rapidly at low values of  $\theta$  and then crosses over the finite size solution and produces negative deviations from it at higher values of  $\theta$ . Fig. 2 compares the shifted solution for  $\theta_s = 0.11$  with that for  $\theta_s = 0.1$ . The percentage error in the shifted point source solution is plotted vs. the center point concentration,  $C^*$ , for the finite size solution. It shows that using  $\theta_s = 0.11$  produces an approximation which is within 1% of the finite size solution for all values of  $C^*$  below 0.37. With  $\theta_s = 0.1$ , the shifted point source solution is within 1% of the finite size solution for all values of  $C^*$  below 0.13. While the ‘overshoot’ approximation undoubtedly is of practical value in some cases, for the present discussion it seems preferable to focus upon the asymptotic solution, which approaches a perfect result at larger values of  $\theta$ .

Choosing  $\theta_s = 0.1$ , Eq. (9) yields  $C_o^* = 2.97$  and Eq. (10) yields  $\sigma_o/a = 0.447$ , at  $\theta = 0$ . Concentration profiles at  $\theta = 0$  for the finite size and the shifted point source

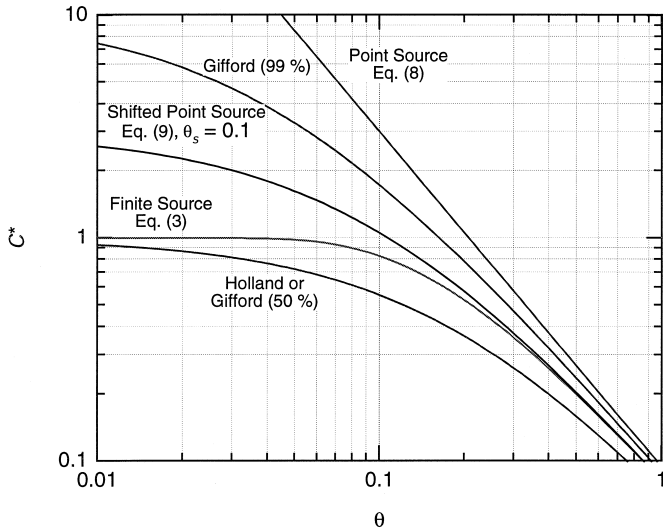


Fig. 1. Spherical puff release.

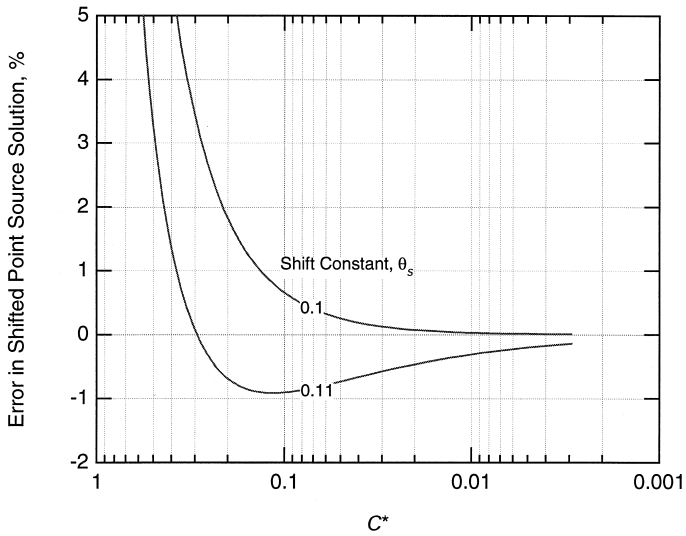


Fig. 2. Effect of  $\theta_s$ .

solutions are compared in Fig. 3. The profiles are obviously of different shape, and the center point concentration given by the shifted point source solution will often be a fictitious value in excess of 100%. But this origin shift,  $\theta_s = 0.1$ , has resulted in the point source solution growing to an effective size which is equal to that of the release of finite size, such that further diffusion will bring the two solutions together in a perfect

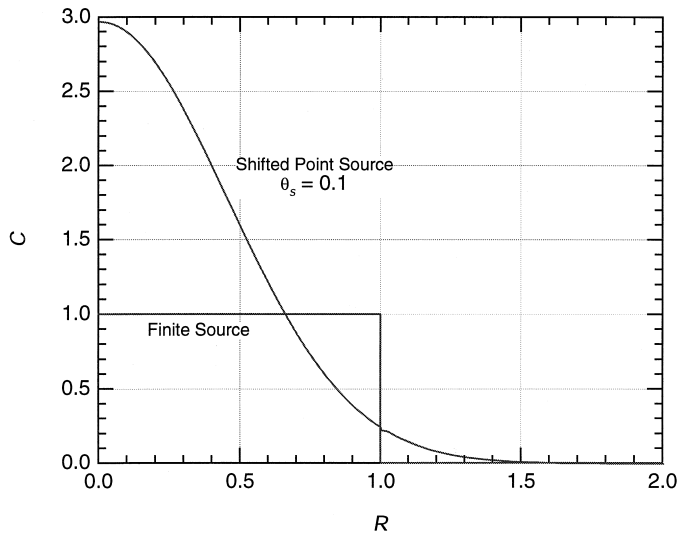


Fig. 3. Concentration profiles at  $\theta = 0$ .

match. In practice, the origin shift is more conveniently described by  $\sigma_0/a$  and  $C_0^*$  than by  $\theta_s$ .

Note that the degree of virtual origin shift recommended here results in  $C_0^* = 2.97$ , not the value of 1.0 suggested by Holland. It follows from Eq. (9) that  $C_0^* = 1$  if  $\theta_s$  is chosen to be 0.207. Inserting this value into Eq. (9) produces a curve in Fig. 1 which shows much greater deviations from the finite source solution than the curve shown for  $\theta_s = 0.1$ .

Integrating the shifted point source solution shown in Fig. 3 results in a value of 82.8% of total moles contained within  $R = 1$ . If Gifford's approach is employed,  $\theta_s = 0.044$  if 99% is chosen, and  $\theta_s = 0.21$  if 50% is chosen. This latter case is very close to the Holland's method. Either choice produces much poorer fit in Fig. 1 than the choice recommended here,  $\theta_s = 0.1$ .

## 2.2. Atmospheric dispersion

Dispersion in the atmosphere occurs by turbulent eddy diffusion, and it shows several deviations from the model just discussed for diffusion with a constant diffusivity. Values of the standard deviation,  $\sigma$ , for experimental results in atmospheric dispersion do not vary as the square root of the dispersion time (or downwind distance) as required by Eq. (5); they vary with the dispersion time to exponents which vary between 0.67 and 0.9, depending on atmospheric stability. This is understood to result from a variation in the effective diffusivity with the size of puff, presumably because there is a spectrum of eddy sizes in the turbulence. Eddies of a size much greater than that of the puff do not dilute the puff by mixing fresh air into it; they simply cause the puff to meander as it travels downwind. But as the puff dilutes and grows in size, further dilution is caused by eddy motions of increasing size, as well as those of the smaller size, and this appears to result in an increase in the effective eddy diffusivity as the puff grows in size. It is assumed that this process can be modeled with reasonable accuracy by a diffusivity which is constant throughout the field but which grows with time as the puff increases in size. Making this assumption, a generalized definition of the dimensionless time,  $\theta$ ,

$$\theta \equiv \frac{1}{a^2} \int_0^t D dt' \quad (11)$$

transforms Eq. (1) to the same form as that for diffusion with a constant diffusivity, and the finite size and point source solutions remain as given in Eqs. (2), (3), (7) and (8). If one could quantitatively relate the diffusivity to the 'size' of the puff at any  $\theta$ , the solution could be completed by relating the diffusion time to the value of  $\theta$  by the inverse of Eq. (11):

$$t = a^2 \int_0^\theta \frac{d\theta'}{D} \quad (12)$$

It has not been possible to conclude whether this effect of a 'size-variable diffusivity' results in a different origin shift than that obtained for the case of a constant diffusivity. If  $\theta_s = 0.1$  is chosen, giving the match-up between the shifted point source solution and the finite size solution shown in Fig. 3, this will be the perfect asymptotic fit and will result in the agreement shown in Fig. 1 if the diffusivities of the shifted point source

solution and the finite size solution remain equal to each other for all values of  $\theta$ . At large values of  $\theta$  the two profiles approach each other very closely, but at low values of  $\theta$  the shapes are quite different and one cannot really know that the eddy diffusivities would be equal. In principle the question could be answered by conducting experiments in the atmosphere with initial releases of ‘top hat’ profiles and Gaussian profiles, but such experiments would be very difficult and have not been conducted. The question might also be addressed by a fundamental approach to turbulent mixing, but no attempt in this direction is made here. Since the origin shift  $\theta_s = 0.1$ , which produces a point source solution with  $\sigma_o/a = 0.447$  and  $C_o^* = 2.97$ , does result in a Gaussian profile which is in some sense the same size as the top hat profile of the finite size release, it is assumed that the eddy diffusivities of the two will be approximately equal and that further dispersion will bring them into coincidence as shown in Fig. 1.

### 2.3. Anisotropic diffusion

Another significant aspect of atmospheric dispersion is that it is anisotropic. Experimental values of the standard deviation,  $\sigma$ , in the vertical direction are approximately half the values in the horizontal direction. This implies that the eddy diffusivity in the vertical direction is approximately one-fourth the eddy diffusivity in the horizontal direction.

Assume that the eddy diffusivity in the downwind direction and that in the crosswind direction are equal but that the eddy diffusivity in the vertical direction is smaller by the factor  $m^2$ :

$$D_x = D_y = \frac{D}{m^{2/3}}; D_z = m^2 \left( \frac{D}{m^{2/3}} \right) = m^{4/3} D \quad (13)$$

and assume further that the  $x$ ,  $y$ , and  $z$  directions are the principal directions for the diffusivity tensor. Note that  $D$  represents the geometric mean of the diffusivities in the  $x$ ,  $y$ , and  $z$  directions.  $D$  might be constant, or it might vary with time, in which case the time transformation should be that shown in Eq. (11). A transformation of the spatial coordinates as

$$\tilde{x} \equiv m^{1/3} x; \tilde{y} \equiv m^{1/3} y; \tilde{z} \equiv \frac{z}{m^{2/3}} \quad (14)$$

transforms Eq. (1) to the same form as that for isotropic diffusion. If the initial condition is a spherical release,

$$x^2 + y^2 + z^2 = a^2 \quad (15)$$

this becomes, in the transformed coordinates, an ellipsoidal release of the same volume

$$(\tilde{x})^2 + (\tilde{y})^2 + (m\tilde{z})^2 = (m^{1/3}a)^2. \quad (16)$$

Therefore, the problem of anisotropic diffusion of a spherical release becomes that of isotropic diffusion of an ellipsoidal release.

This problem has been solved numerically by a finite-difference method which is an extension of the methods of Peaceman and Rachford [6] and Brian [7]. The partial

differential equation for diffusion was written in cylindrical coordinates to take advantage of the symmetry of this problem about the  $z$  axis and therefore to simplify the finite-difference solution to one in two spatial dimensions and time. Convergence of the solution was confirmed by refining the grid and also by comparing the solution for  $m = 1$  with the analytical solution for isotropic diffusion of a spherical release, Eq. (3). An infinite series solution was also developed, and it confirmed the accuracy of the finite-difference solution. Fig. 4 shows a plot of the center point concentration,  $C^*$ , vs. dimensionless time,  $\theta$ , for values of  $m = 1, 0.6, 0.5, 0.4$  and  $0.25$ . It is seen that  $C^*$  declines more rapidly as the value of  $m$  is decreased. Remembering that the dimensionless time is defined in terms of the geometric mean of the diffusivities in the  $x, y$  and  $z$  directions, it might not have been anticipated that the system would respond more quickly with increasing anisotropy of the diffusivity tensor. On the other hand, interpreting Fig. 4 as the isotropic diffusion of ellipsoidal releases, it would be expected that the response would become faster as the shape of the release departs more and more from spherical and therefore as the surface area increases. The curve for  $m = 2$  is not shown in Fig. 4 but lies close to the curve for  $m = 0.5$ .

Values of  $\theta_s$  were calculated for the anisotropic diffusion cases in the same manner as was displayed in Table 1 for the isotropic case. Values of  $C^*$  obtained from the finite-difference calculations and from the infinite series solution at various values of  $\theta$  were substituted into Eq. (9) to yield values of  $\theta_s$ . These values asymptotically approached a constant at large values of  $\theta$ , and these asymptotes are shown in Table 2. Using these values of  $\theta_s$  and taking  $\theta = 0, \sigma_o/a$  and  $C_o^*$  were calculated from Eqs. (10) and (9), respectively and are also shown in the table. In this case,  $\sigma$  represents the geometric mean of  $\sigma_x, \sigma_y,$  and  $\sigma_z$ . Table 2 describes the increasing time shift required as the  $z$  direction diffusivity departs more and more from the horizontal diffusivities. These values are shown graphically in Fig. 5.

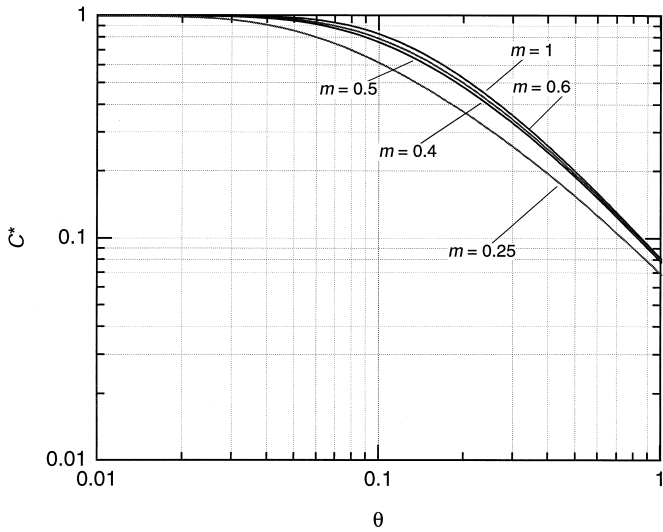


Fig. 4. Effect of diffusivity ratio spherical puff release.



Table 2  
Virtual origin shift spherical puff release

$m$	$\theta_s$	$\sigma_o / a$	$C_o^*$
0.25	0.238	0.690	0.810
0.3	0.196	0.626	1.08
0.4	0.149	0.546	1.63
0.5	0.126	0.502	2.10
0.6	0.113	0.475	2.48
1	0.1	0.447	2.97
2	0.119	0.488	2.29

To apply these results to atmospheric dispersion, Fig. 5 should be used in order to determine the appropriate virtual origin shift for the point source dispersion model. The conventional point source model for a nonbuoyant release of negligible momentum is

$$c = \frac{Q}{(2\pi)^{3/2} \sigma_x \sigma_y \sigma_z} \exp\left(-\left[\frac{x^2}{2\sigma_x^2} + \frac{y^2}{2\sigma_y^2} + \frac{z^2}{2\sigma_z^2}\right]\right), \tag{17}$$

$$c^* = \frac{Q}{(2\pi)^{3/2} \sigma_x \sigma_y \sigma_z}, \tag{18}$$

in which values of  $\sigma_x$ ,  $\sigma_y$ , and  $\sigma_z$  vs. downwind distance from the point source origin are available in the literature [3,8–10]. For a spherical release of finite radius,  $a$ , one must find the downwind distance from the point source origin at which  $(\sigma_x \sigma_y \sigma_z)^{1/3}$  divided by  $a$  matches the value of  $\sigma_o/a$  read from Fig. 5 at the appropriate value of  $m$ .

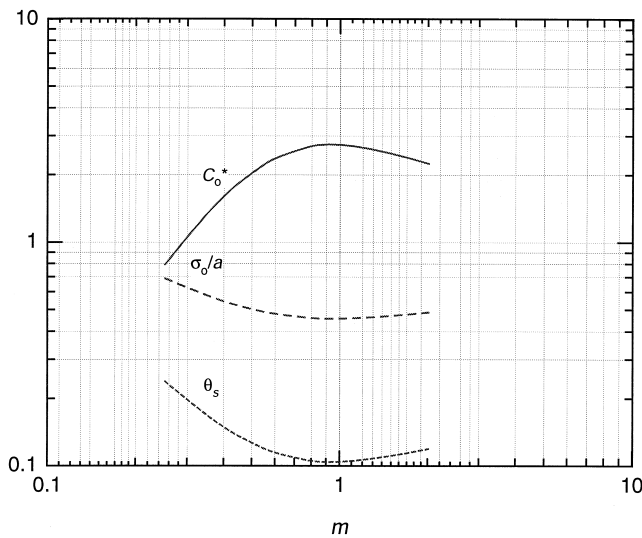


Fig. 5. Virtual origin shift spherical puff release.

This is the downwind distance from the point source origin to the origin of the release of finite size. The value of  $m$  employed in reading Fig. 5 is given by

$$m = \sigma_z / \sigma_y. \quad (19)$$

Since correlations [3,9] of  $\sigma$  values for atmospheric dispersion produce values of  $m$  which vary with downwind distance as well as with weather stability, it is recommended that the value of  $m$  to be employed in reading Fig. 5 should be evaluated at the origin of the release of finite size.

#### 2.4. Releases of nonspherical shape

The results shown above were for an initial release in which the concentration of the pollutant was uniform at the value  $c_0$  throughout the sphere described by Eq. (15). Consider the case in which the initial release shape is ellipsoidal instead of spherical:

$$x^2 + y^2 + (\alpha z)^2 = (\alpha^{1/3} a)^2. \quad (20)$$

The volume of this ellipsoid is the same as that of the sphere described by Eq. (15). For anisotropic diffusion, the transformation of spatial coordinates given by Eq. (14) transforms the initial condition to that of a different ellipsoid:

$$\tilde{x}^2 + \tilde{y}^2 + (m\alpha\tilde{z})^2 = (m^{1/3}\alpha^{1/3}a)^2. \quad (21)$$

The solution, in the transformed coordinates, to the diffusion problem is now seen to be the same as that obtained earlier in which  $m$  is now replaced by  $m\alpha$ .

#### 2.5. Steady continuous release

For a steady continuous release, axial diffusion is negligible, and the problem is one of diffusion in the  $y$  and  $z$  directions. For isotropic diffusion with a constant diffusivity and with an initial concentration which is uniformly equal to  $c_0$  over a circle,

$$y^2 + z^2 = a^2 \quad (22)$$

the solution given by Carslaw and Jaeger [11] can be simplified to the form:

$$C = \int_0^\infty e^{-\theta u^2} J_0(uR) J_1(u) du. \quad (23)$$

For the center point concentration at  $R = 0$ ,

$$C^* = 1 - \exp\left(-\frac{1}{4\theta}\right). \quad (24)$$

The point source solution corresponding to an initial condition in which the concentration is infinite throughout a point source of zero size, is given by

$$c = \frac{\gamma}{2\pi\sigma^2} \exp\left(-\frac{r^2}{4\sigma^2}\right) \quad (25)$$

in which

$$\gamma \equiv \int_0^\infty \int_0^\infty c \, y \, dz. \quad (26)$$

For a steady release at the rate of  $\dot{Q}$  into the atmosphere in which the wind velocity is  $V$ ,

$$\gamma = \frac{\dot{Q}}{V} \tag{27}$$

and therefore  $\gamma$  is constant with time (or downwind distance). Taking  $\gamma$  to be the same value as that in the finite size release

$$\gamma = \pi a^2 c_o \tag{28}$$

and using Eq. (5), which does apply, Eq. (25) becomes

$$C = \frac{1}{4\theta} \exp\left(-\frac{R^2}{4\theta}\right). \tag{29}$$

At  $R = 0$ ,

$$C^* = \frac{1}{4\theta}. \tag{30}$$

Employing a shift in the point source origin, the shifted point source solution becomes

$$C^* = \frac{1}{4(\theta + \theta_s)}. \tag{31}$$

Expanding Eq. (24) in a series reveals an asymptotic fit with Eq. (31) with the choice  $\theta_s = 1/8$ .

Fig. 6 shows a comparison of the point source model, the shifted point source model, and the finite size model. As in the case of a puff release, the shifted point source model

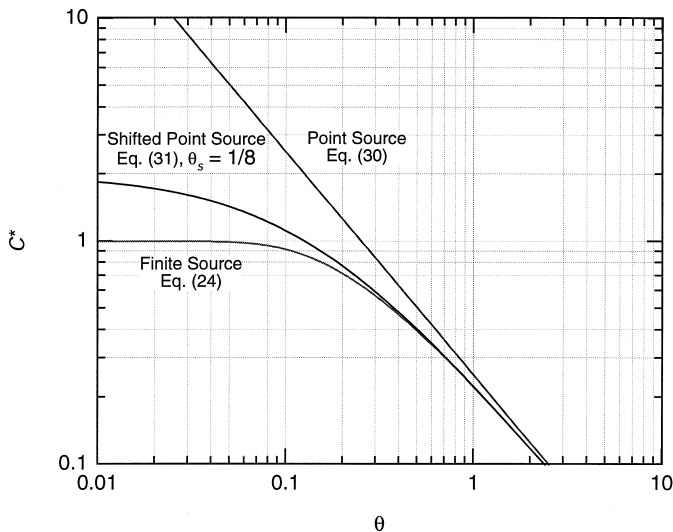


Fig. 6. Continuous release.

can be seen to represent a substantial improvement in the intermediate and far fields. Using  $\theta_s = 1/8$ , Eq. (10) yields  $\sigma_o/a = 0.5$  and Eq. (31) yields  $C_o^* = 2.0$ , at  $\theta = 0$ .

The considerations regarding deviations of atmospheric dispersion from the model of diffusion with a constant diffusivity are similar to those discussed earlier for the puff release. Regarding the eddy diffusivity increase as the size of the plume increases, the conclusions are the same. Regarding anisotropic diffusion, assume that the diffusivities are given by

$$D_y = \frac{D}{m}; D_z = m^2 \left( \frac{D}{m} \right) = mD. \tag{32}$$

A transformation of the spatial coordinates as

$$\tilde{y} \equiv m^{1/2} y; \tilde{z} \equiv z/m^{1/2} \tag{33}$$

transforms Eq. (1) to the same form as that for isotropic diffusion. If the initial condition is a constant composition over the cross section of the circle of Eq. (22), this gets transformed to an ellipse of the same area:

$$(\tilde{y})^2 + (m\tilde{z})^2 = (m^{1/2}a)^2. \tag{34}$$

The problem of diffusion in the  $\tilde{y}$  and  $\tilde{z}$  directions with an initial condition of constant composition within the ellipse given by Eq. (34) has been solved by a finite-difference method similar to that mentioned earlier, and an infinite series solution was also developed. The results are presented in Fig. 7.

The results in Fig. 7 for a continuous release are similar to those shown in Fig. 4 for a puff release. As the value of  $m$  departs from unity, the center point concentration declines more rapidly. In this case, reciprocal values of  $m$  give identical results. Asymptotic values of  $\theta_s$  obtained from the finite difference and infinite series solution

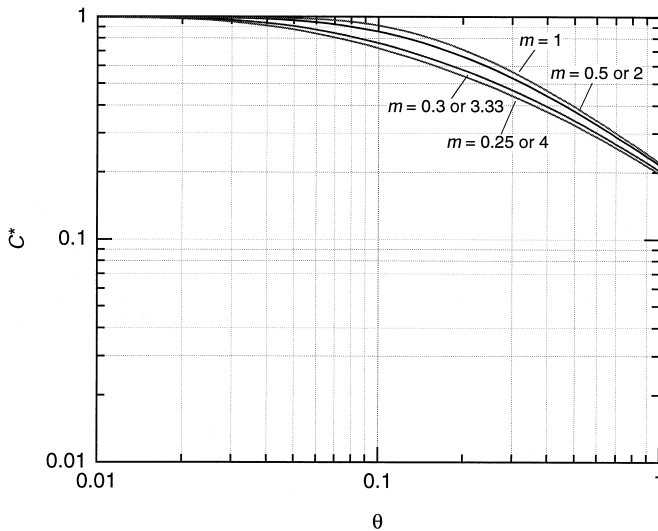


Fig. 7. Effect of diffusivity ratio continuous release.

Table 3  
Virtual origin shift continuous release

$m$	$\theta_s$	$\sigma_o/a$	$C_o^*$
0.25 or 4	0.266	0.729	0.94
0.3 or 3.333	0.225	0.671	1.11
0.4 or 2.5	0.180	0.600	1.39
0.5 or 2	0.154	0.555	1.62
0.6 or 1.666	0.141	0.531	1.77
1	0.125	0.500	2.00

are presented in Table 3 and shown graphically in Fig. 8. Corresponding values of  $\sigma_o/a$  and  $C_o^*$  are also shown. Note that  $\sigma$  represents the geometric mean of  $\sigma_y$  and  $\sigma_z$ . The value of  $\sigma_o/a$  varies from 0.5 at  $m = 1$  to 0.729 at  $m = 1/4$  or 4. For rectangular releases, Bowers et al. [4] recommend a single value 0.47, irrespective of  $m$ , for the ratio of  $\sigma_o$  to half the rectangle side.

For the steady release of a pollutant at the rate  $\dot{Q}$  into the atmosphere with a wind velocity  $V$  and with negligible buoyancy and initial momentum, the point source dispersion model is given by

$$c = \frac{\dot{Q}}{2\pi V\sigma_y\sigma_z} \exp\left(-\left[\frac{y^2}{2\sigma_y^2} + \frac{z^2}{2\sigma_z^2}\right]\right), \tag{35}$$

$$c^* = \frac{\dot{Q}}{2\pi V\sigma_y\sigma_z} \tag{36}$$

in which values of  $\sigma_y$  and  $\sigma_z$  vs. distance downwind from the point source origin are given in Turner [3] and van Buijtenen [9]. To apply the results of this study, Fig. 8

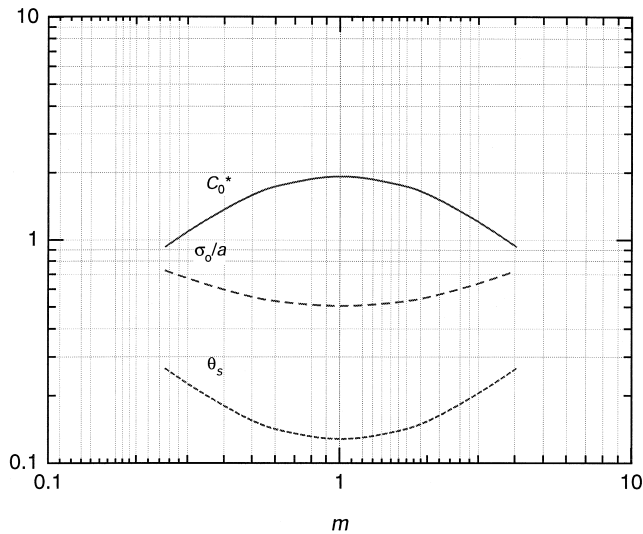


Fig. 8. Virtual origin shift continuous release.

should be used in order to determine the appropriate virtual origin shift for the point source dispersion model. For the steady release at the rate  $\dot{Q}$  in which the initial condition corresponds to uniform concentration,  $c_o$ , within a circle of radius  $a$ , one must find the downwind distance from the point source origin at which  $(\sigma_y \sigma_z)^{1/2}$  divided by  $a$  matches the value of  $\sigma_o/a$  read from Fig. 8 at the appropriate value of  $m$ . This is the downwind distance from the point source origin to the origin of the release of finite size. The value of  $m$  to be employed in reading Fig. 8 is given by Eq. (19), evaluated at the origin of the release of finite size.

### 3. Example problem

The application of these results will be illustrated by a simple example involving a spherical puff release with a radius of 15 m. Initial momentum and buoyancy will be assumed to be negligible, and it will be assumed that the release is at a sufficient elevation such that interference by the ground need not be considered. It is desired to calculate the downwind distance at which the centerpoint concentration has been reduced to a value of 1/10 of the concentration of the spherical release. It is assumed that the weather is stable, Class E. Following the recommendation in Ref. [10],  $\sigma_x$  will be assumed to be equal to  $\sigma_y$ , and the correlation in van Buijtenen [9] will be used:

$$\sigma_x = \sigma_y = 0.098d^{0.902}, \quad (37)$$

$$\sigma_z = 0.15d^{0.73}. \quad (38)$$

From this it follows that:

$$\sigma = (\sigma_x \sigma_y \sigma_z)^{1/3} = 0.1129d^{0.8447}, \quad (39)$$

$$m = \frac{\sigma_z}{\sigma_y} = 1.5306d^{-0.172} \quad (40)$$

in which all lengths are measured in meters. From Eq. (39) it follows that,

$$\frac{\sigma}{a} = 0.00753d^{0.8447} \quad (41)$$

since the radius of the sphere is 15 m. Choosing various values of  $d$ , Eqs. (40) and (41) can be solved to generate a curve of  $\sigma/a$  vs.  $m$ , and the intersection of this curve with the curve in Fig. 5 produces the desired solution. By trial and error, the intersection corresponds to  $d_o = 134$  m, at which  $\sigma/a = 0.47$  and  $m = 0.66$ . Therefore, the point source release is taken to be 134 m upwind of the actual spherical puff release. Combining Eqs. (6) and (18) gives,

$$C^* = \frac{\sqrt{2/\pi}/3}{\sigma_x \sigma_y \sigma_z / a^3} = \frac{\sqrt{2/\pi}/3}{(\sigma/a)^3} \quad (42)$$

From this, it follows that  $C^* = 0.1$  when  $\sigma/a = 1.385$ . Using Eq. (41), this corresponds to  $d = 480$  m, which is the downwind distance from the point source origin to the point

at which  $C^* = 0.1$ . This corresponds to  $d - d_0 = 346$  m, which is the downwind distance from the actual origin of the puff release and is therefore the desired result.

#### 4. Nomenclature

$a$	radius of sphere or circle
$c$	concentration of pollutant, moles/m <sup>3</sup>
$C$	$c/c_0$
$d$	downwind distance from origin of release to center of puff or plume, m
$D$	diffusivity, m <sup>2</sup> /s
$J_0$	Bessel function of the first kind, of order 0
$J_1$	Bessel function of the first kind, of order 1
$m$	$\sqrt{D_z/D_y}$ ; also $\sigma_z/\sigma_y$
$Q$	quantity of pollutant released in puff, moles
$\dot{Q}$	rate of continuous release of pollutant, moles/s
$r$	$\sqrt{x^2 + y^2 + z^2}$ for puff; $\sqrt{y^2 + z^2}$ for continuous release, m
$R$	$r/a$
$t$	time of dispersion ( $= d/V$ ), s
$u$	integration variable
$V$	wind velocity, m/s
$x$	horizontal downwind distance from plume center, m
$y$	horizontal crosswind distance from plume center, m
$z$	vertical distance from plume center, m
$\tilde{x}, \tilde{y}, \tilde{z}$	puff—Eq. (14); continuous—Eq. (33)

#### Greek

$\alpha$	eccentricity factor for ellipse, Eq. (20)
$\gamma$	defined by Eq. (26), moles/m
$\sigma$	standard deviation—see Eqs. (4), (16) and (35), m
$\theta$	dimensionless time $\equiv Dt/a^2$ , or defined by Eq. (11) when $D$ varies with $t$
$\theta_s$	virtual origin shift—Eqs. (9) and (31)

#### Subscripts

$o$	$t = 0$
$x, y, z$	$x, y, z$ directions

#### Superscripts

*	center of plume
,	dummy variable of integration

#### Acknowledgements

The authors gratefully acknowledge Prof. Kenneth A. Smith at MIT and Mr. Louis C. Doelp for their helpful discussions and comments.

## References

- [1] J.Z. Holland, A meteorological survey of the Oak Ridge area, Report ORO-99, Oak Ridge National Lab., November 1953, p. 539.
- [2] F. Gifford Jr., *J. Meteorol.* 12 (1955) 245.
- [3] B. Turner, Workbook of Atmospheric Dispersion Estimates, Public Health Service, Publication 999-AP-26, Robert A. Taft Sanitary Engineering Center, Cincinnati, OH, 1967.
- [4] J.F. Bowers, J.R. Bjorklund, C.S. Cheney, Industrial Source Complex (ISC) Dispersion Model User's Guide, Vol. I, Publication No. EPA-450/4-79-030, U.S. Environmental Protection Agency, Research Triangle Park, NC, 1979.
- [5] S. Carslaw, J.C. Jaeger, *Conduction of Heat in Solids*, 2nd edn., Oxford Univ. Press, 1990, p. 257.
- [6] W. Peaceman, H.H. Rachford, *SIAM J.* 3 (1955) 28.
- [7] P.L.T. Brian, *AIChE J.* 7 (1961) 367.
- [8] R. Hanna, G.A. Briggs, R.P. Hosker, Jr., *Handbook on Atmospheric Diffusion*, DOE/TIC-11223, DOE, 1982.
- [9] J.P. van Buijtenen, *J. Hazardous Mater.* 3 (1980) 201.
- [10] Center for Chemical Process Safety, *Guidelines for Vapor Cloud Dispersion Models*, 2nd edn., American Institute of Chemical Engineers, New York, NY, 1996.
- [11] S. Carslaw, J.C. Jaeger, *Conduction of Heat in Solids*, 2nd edn., Oxford Univ. Press, 1990, p. 346.